I_{sp} and C_F were the same since $\dot{m}$ is unaffected by the nonisentropic effects. The identical trends exhibited by flow models 2 and 3 lend great support to the methods and results obtained in this study.

Conclusions

In any actual rocket motor, effects not included here are present which would tend to change the results somewhat. However, the trends illustrated by the results presented herein for an arbitrary nonisentropic process should be useful in gaining insight into the coupled effects of C_c, η, α, γ, and r_o on conical nozzle performance and design. The most significant conclusion reached in this study is that in real systems subject to nonisentropic flow effects, maximum performance always requires some finite amount of underexpansion and a correspondingly smaller area ratio than does isentropic expansion.

References

[1] Durham, F. P., "Thrust Characteristics of Underexpanded Nozzles," *Jet Propulsion*, Vol. 25, No. 12, Dec. 1955, pp. 696–700.

[2] Rowe, P. N., "The Thrust of a Supersonic Conical Nozzle with Non-Isentropic Flow," *Proceedings of the Institution of Mechanical Engineering*, Vol. 172, No. 30, 1958, pp. 877–888.

[3] Scofield, M. P. and Hoffman, J. D., "Optimization of Conical Thrust Nozzles," *Journal of Spacecraft and Rockets*, Vol. 4, No. 11, Nov. 1967, pp. 1547–1549.

[4] Landsbaum, E. M., "Thrust of a Conical Nozzle," *ARS Journal*, Vol. 29, No. 3, March 1959, pp. 212–213.

[5] Malina, F. J., "Characteristics of the Rocket Motor Unit Based on the Theory of Perfect Gases," *Journal of the Franklin Institute*, Vol. 230, 1940, pp. 433–454.

[6] Rao, G. V. R., "Evaluation of Conical Nozzle Thrust Coefficient," *ARS Journal*, Vol. 29, No. 8, Aug. 1959, pp. 606–607.

[7] Sauer, R., "General Characteristics of the Flow Through Nozzles at Near Critical Speeds," TM 1147, June 1947, NACA.

[8] Hall, I. M., "Transonic Flow in Two-Dimensional and Axially Symmetric Nozzles," *Quarterly Journal of Mechanics and Applied Mathematics*, Vol. XV, Pt. 4, 1962, pp. 487–508.

Ablative Materials for Controlled High Regression Rates in Rocket Motors

H. O. Davis* and H. M. Evensen†
Aerojet-General Corporation, Sacramento, Calif.

THE conventional method of obtaining a neutral pressure curve in a solid rocket motor involves special, and at times, complex grain designs. Tactical rocket motors operating at high pressures with high burning rate propellants are subjected to high-acceleration loads which impose structural limitations on propellant grain configurations. The simplest grain, from a structural point of view, is an internal burning cylinder that would produce a progressive pressure curve. By combining this with a nozzle throat area increase at a rate proportional to the mass flow rate increase caused by surface area increase, an essentially neutral pressure curve can be obtained. Thus, there is no further increase in r_b due to P_c change (which would compound the acceleration problem).

Regression rates can be varied by affecting changes in the individual ablative material. However, the regression required for the Zero Antiaircraft Potential (ZAP) motor‡ appeared to be beyond the scope of any variation in the standard ablatives such as carbon, silica, or asbestos reinforcement since a regression rate of approximately 0.30 in./sec was needed. It was unlikely that a standard material could be tailored to produce a regression rate of this magnitude. Furthermore, a low density or resin modification significant enough to achieve the desired increase would likely produce nonuniformities and erratic performance. The highest regression obtained for a standard carbon phenolic had been 0.018/sec for a similar pressure and environment as the ZAP motor. Two general categories of materials were considered: 1) single component: melt formers (e.g., aluminum) and sublimers (e.g., polytetrafluoroethylene); 2) composite materials.

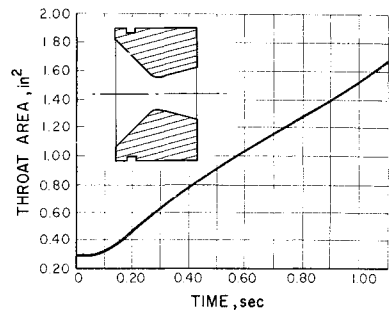

Fig. 1 Throat area-time function for ZAP nozzle material evaluation in 3KS-1000 motor (inset-test nozzle configuration).

Within the composite materials, three basic resin systems were considered: polyesters, epoxies, and phenolics. Reinforcements considered include a wide range of thermoplastic and thermosetting materials, entailing melt formers, sublimers, and char formers. The thermoplastics are primarily reduced to decomposition gases and leave very little residue. Thermosetting materials decompose, leaving various amounts of residue depending on the polymer structure.

From data in Ref. 1, it appeared that glass and nylon-reinforced phenolics would be candidates.

Compatibility with the propellant exhaust gases was considered to the extent that if oxidation was to be the controlling mechanism of material removal, a low char density would be required. The mechanical removal of a low-density char was also a method of achieving a high regression rate. A low melt temperature in conjunction with a low viscosity offered still another mechanism. These analyses had to be qualitative because of the lack of empirical data and the lack of comparative test conditions. Availability and cost were also important, of course.

Subscale Screening Tests

A subscale motor identified as 3KS-1000, used primarily for propellant evaluation, was selected as the test vehicle for evaluating the candidate materials. The throat insert configuration is shown in Fig. 1. The motor was designed to have an average chamber pressure ($\bar{P}_c$) of about 2000 psi.

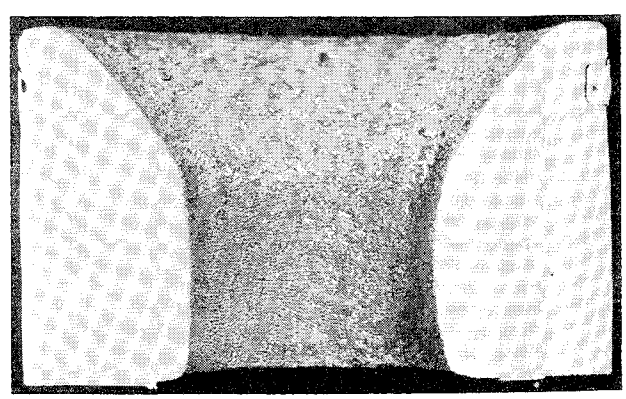

Fig. 2 Postfire photograph of a cross section from nylon/phenolic with 50% resin content.

Presented as Paper 69-423 at the AIAA 5th Propulsion Joint Specialist Conference, U.S. Air Force Academy, Colo., June 9–13, 1969; submitted June 16, 1969; revision received August 18, 1969.

* Engineering Specialist.

† Supervisor. Member AIAA.

‡ Developed under Contract N60921-68-C-0225.

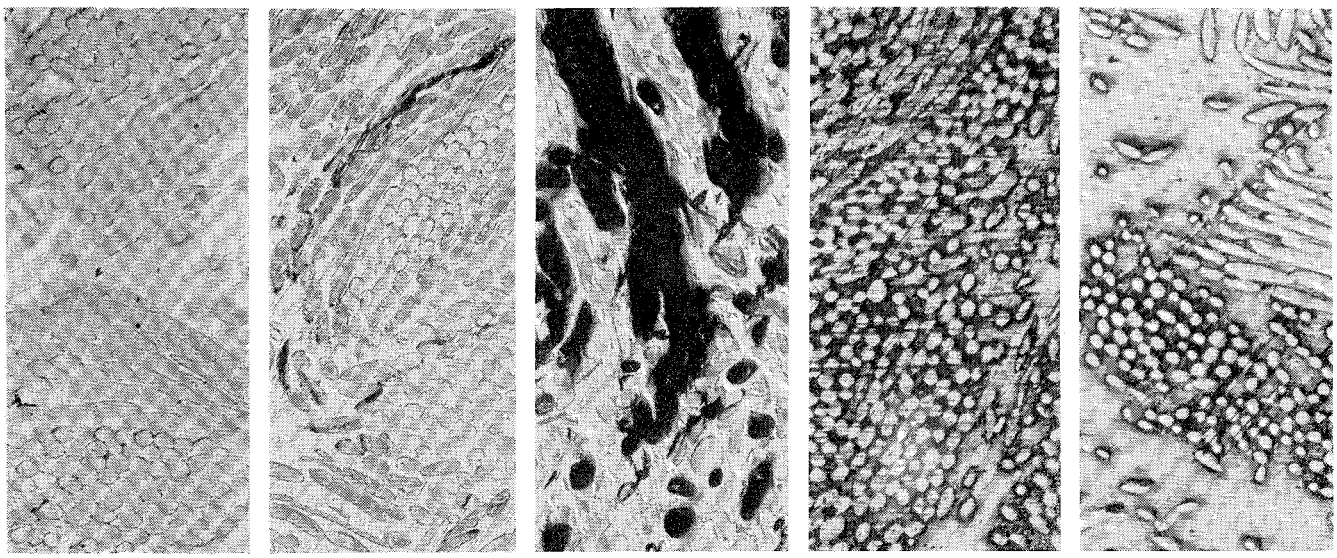

a) 50% phenolic b) 30% phenolic c) Staple fiber 50% phenolic d) 47% epoxy novolac e) 56% epoxy novolac

Fig. 3 Photomicrographs of nylon-reinforced composites with various percentages of resin.

One of the early firings was a chopped nylon-reinforced phenolic that produced the desired regression rate. It was calculated that a 0.36 in./sec regression rate in the subscale motor would produce a 0.30 in./sec rate in the full-scale ZAP motor. After the early success of achieving the required regression, the firing test schedule plan was changed to evaluate small changes in the nylon composite system rather than test the broad categories of materials previously selected. The materials tested other than the nylon-reinforced composites were: aluminum, TiO_2/epoxy, and glass/epoxy. The aluminum was the only melt former tested. (Polytetrafluoroethylene was not tested.) The aluminum and TiO_2/epoxy failed almost catastrophically, leaving no residual material. As a result of an equipment malfunction, the glass epoxy results were not obtained; however, it appeared that the regression rate ($\dot{r}$) would have been much too low. The nylon-reinforced composite test results are listed in Table 1.

The $\dot{r}$ data show considerable scatter, outside the range expected by variations in P_c. This was attributed to material and/or process differences. An example of the plots generated to determine throat area change vs time is shown in Fig. 1. The plots were used to establish a "steady-state regression rate" and were generally in good agreement (within 10%) with the average regression determined from measured erosion depth and firing duration. One firing (not shown in Table 1) had 37% phenolic resin and 5% aluminum filler.

Table 1 Regression rates for nylon-reinforced composites—subscale test

Resin Type	Resin %	T_i, °F	$\bar{P}_c$, psia	T_{test}, sec	$\dot{r}$, in./sec
Phenolic	52.5	−65	1703	1.23	0.271
	52.5	80	2138	0.96	0.355
	52.5	+160	2203	0.90	0.402
	48	−65	1482	1.22	0.306
	48	80	1548	0.94	0.336
	48	+160	1990	0.95	0.424
	48	80	2176	0.97	0.333
	44[a]	80	2374	0.90	0.323[b]
	40	80	2215	0.96	0.331
	30	80	1823	1.15	0.380[b]
Epoxy novolac	56	80	1148	1.19	0.432
	47	80	1260	1.22	0.432

[a] Reinforcement in staple fiber form.
[b] Spallation with irregular surface.

The data were not reduced because of a malfunction; however, the qualitative evaluation indicated a lower regression rate than the standard system.

Postfire Evaluation

Five of the candidate materials tested in the subscale motor were sectioned and photographed. The material system that gave the required regression rate was the nylon/phenolic with a 50 ± 3% resin content. The cross section of a typical postfire throat is shown in Fig. 2. The regression surface is smooth and uniform.

The regression was nonuniform for the nylon/phenolic with 30% resin. Spallation (chunking) occurred in several places. The mechanism is assumed to be virgin material cracking and ejecting.

The surface of the nylon/epoxy novolac with 47% resin had small pits in the flame surface; however, the material loss was uniform. The appearance of the nylon/epoxy novolac with 56% resin was almost identical to the nylon/epoxy novolac with 47% resin except that the 56% did not appear to have flowed at the surface as much. The nylon/epoxy novolac composite displayed sufficiently uniform regression to be considered a candidate if higher regression rates were required.

Figure 3 shows 100X photomicrographs of the 5 materials sectioned. Figure 3a shows the nylon/phenolic with a 50 ± 3% resin content. There are resin pockets between and within fiber bundles. A lower percent resin content for this material appears feasible. Figure 3b shows the nylon/phenolic with 30% resin content. The resin to reinforcement distribution was uniform with almost no resin pockets. The cracks which appear as black streaks in the photomicrograph were typical for this nozzle section. Figure 3c shows the staple nylon fiber/phenolic. The voids and cracks which appear black in the photomicrograph were characteristic of this material. The nylon/epoxy novolac with 47% resin appears to have uniform distribution of fibers with very few resin pockets (Fig. 3d), whereas the nylon/epoxy novolac with 56% resin (Fig. 3e) has larger resin pockets.

The materials shown with the cracks (Figs. 3b and 3c) were the only materials which had erratic nonuniform regression. Cracks prior to firing and/or during firing are potential cause for nonuniform performance and materials that exhibit this characteristic could not be used. Nondestructive testing of nozzle throat components to insure that there are no cracks is required.

Full-Scale ZAP Rocket Motor Firings

A total of 19 full-scale motors with nylon/phenolic nozzle throat inserts were statically test fired. The performance of the nylon/phenolic throat inserts was satisfactory; however, two distinct groupings of erosion rates could be established. Because of limited funding the material was not fully characterized for this program and more than one lot of material was used. However, the material performance within each group was very uniform, and there was no evidence of any spalling or chunking. Apparently, the thermochemical or mechanical response for each "group" of material is sufficiently different to produce measured difference in regression. Additional analysis would be required to ascertain the cause for the difference in performance. Selected material property measurements and perhaps a theoretical model of material behavior would be needed to make the differences predictable.

References

[1] Katsikas, D. J., Castel, G. K., and Higgins, J. S., "Ablation Handbook Entry Materials Data and Designs," AFML-TR-66-262, Nov. 1966, Air Force Materials Lab., Wright-Patterson Air Force Base, Ohio, pp. 401–439.

Rocket Combustion Stability Monitoring by Temporal Radiometry

W. F. Herget,* R. L. Proffit,† and J. E. Witherspoon‡
Rocketdyne, A Division of North American Rockwell Corporation, Canoga Park, Calif.

Discussion

THE diagnosis of combustion instability in rocket engines requires knowledge of the frequency, amplitude, and phase of the chamber pressure variations. The measurement techniques usually relied upon to obtain these data employ high-frequency response pressure transducers and/or accelerometers, or, in specially designed transparent chambers, streak photography. Although the more meaningful measurements are obtained with flush-mounted chamber pressure transducers, this measurement is difficult, if not impossible, to obtain on tubular-walled chambers, and such a transducer is often the time-limiting component in workhorse chambers. Feed system measurements and accelerometers often do not give a true reflection of the pressure oscillations in the combustion chambers, or may be difficult to interpret.

The use of temporal or a.c. radiometry allows the determination of chamber pressure oscillations without physical attachment of measurement equipment to the engine, since the radiometer may be situated at any convenient distance from the test stand. The concept of a.c. radiometry is not new (see, e.g., Ref. 1). In the past few years, however, several fundamental guides to successful employment of the technique have been established so that reliable, semiroutine measurements can be obtained.

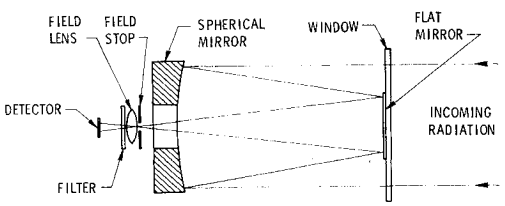

Fig. 1 Schematic of radiometer optical system.

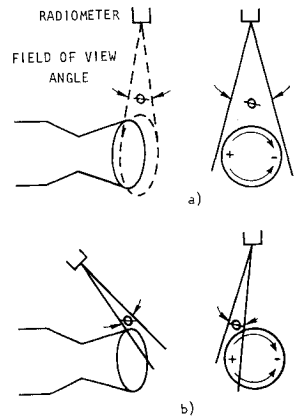

Fig. 2 Effect of radiometer field of view.

Frequency analysis of the time-varying radiation from rocket plumes has shown that this radiation is of two types: 1) a continuous frequency distribution, possessing an f^{-n} dependence caused by random processes, and 2) discrete frequencies caused by oscillations in combustion chamber pressure. Measurements made on engines using a variety of propellants have shown excellent agreement between a.c. radiometry and flush-mounted, high-speed pressure transducers, both in frequency and in spatial phasing.

A typical a.c. radiometer consists of an optical system to focus electromagnetic radiation from the engine exhaust plume onto a detector, a field stop to limit the field of view (FOV) of the radiometer to a particular spatial region of the exhaust, and spectral filters that allow only selected wavelengths to reach the detector (Fig. 1). An uncooled PbSe detector is used to monitor near infrared (1–6μ) radiation, and a photomultiplier tube is used to monitor ultraviolet or visible radiation. The detector output is usually recorded at several levels of amplification on separate channels of an FM tape recorder to provide accuracy over a wide intensity range. Typical frequency response is as high as 20,000 Hz. Other channels of the tape may be used for timing information and other desired measurements. Primary data reduction is carried out on a commercial frequency analyzer. The reduced data consist of a "sonagram" displaying frequency and relative intensity as a function of time. Wave forms and phase relationships may be studied with a conventional oscilloscope.

The field stop is used because if the radiometer FOV was such that both high and low regions of radiation intensity are viewed simultaneously, the integrated a.c. intensity may be zero. For example, if the radiometer views the entire plume (as in Fig. 2a), only the radial and longitudinal acoustic modes may be detected, because the tangential modes will be effectively integrated at any instant of time. To observe tangential modes, only a small portion of the nozzle exit (along the edge of the plume) is viewed (Fig. 2b). To identify all possible acoustic modes, it may be necessary to have as many as

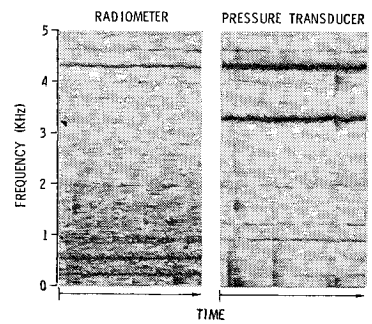

Fig. 3 Sonograms of radiometer (10° FOV) and pressure transducer data.

Presented as Paper 69-580 at the AIAA 5th Propulsion Joint Specialist Conference, Colorado Springs, Colo., June 9–13, 1969; submitted June 16, 1969; revision received August 15, 1969.

* Member of the Technical Staff, Mechanics and Optics, Research.
† Principal Scientist, Mechanics and Optics, Research.
‡ Principal Scientist, Measurements and Instruments, Research. Associate Fellow AIAA.